
Article:
Chen, S., Li, W., Wu, J. et al. (9 more authors) (2016) Electrically pumped continuous-wave III–V quantum dot lasers on silicon. Nature Photonics, 10. pp. 307-311. ISSN 1749-4885

https://doi.org/10.1038/nphoton.2016.21

Electrically Pumped Long Lifetime Continuous-Wave III-V Quantum-Dot Lasers Directly Grown on Silicon Substrates

Siming Chen[1]*, Wei Li[2], Jiang Wu[1], Qi Jiang[1], Mingchu Tang[1], Samuel Shutts[3], Stella N. Elliott[3], Angela Sobiesierski[3], Alwyn J. Seeds[1], Ian Ross[2], Peter M. Smowton[3], and Huiyun Liu[1]*

Reliable, efficient electrically pumped silicon-based lasers would enable full integration of photonic and electronic circuits, but have previously only been realized by wafer bonding. Here, we demonstrate the first continuous-wave InAs/GaAs quantum-dot lasers directly grown on silicon substrates with a low threshold current density of 62.5 A/cm^2, a room-temperature output power exceeding 105 mW, lasing operation up to 120 ^{o}C, and over 3,100 hours of continuous-wave operating data collected, giving an extrapolated mean time to failure of over 100,158 hours. The realization of high-performance quantum-dot lasers on silicon is due to the achievement of a low density of threading dislocations on the order of 10^5 cm^{-2} in the III-V epilayers by combining a nucleation layer and dislocation filter layers with *in-situ* thermal annealing. These results are a major advance towards silicon-based photonics and photonic-electronic integration, and could provide a route towards reliable and cost-effective monolithic integration of III-V devices on silicon.

Increased data throughput between silicon processors in modern information processing demands unprecedented bandwidth and low power consumption beyond the capability of conventional copper interconnects. To meet these requirements, silicon photonics has been under intensive study in recent years[1,2]. Despite rapid progress being made in silicon-based light modulation and detection technology and low-cost silicon optoelectronic integrated devices enabled by the mature CMOS technology[3,4], an efficient reliable electrically pumped laser on a silicon substrate has remained an unrealized scientific challenge[5]. Group IV semiconductors widely used in integrated circuits, e.g. silicon and germanium, are inefficient light-emitting materials due to their indirect bandgap, introducing a major barrier to the development of silicon photonics. Integration of III–V materials on a silicon platform has been one of the most promising techniques for generating coherent light on silicon. III–V semiconductors with superior optical properties, acting as optical gain media, can be either bonded or epitaxially grown on silicon substrates[6-11], with the latter approach being more attractive for large scale, low-cost, and streamlined fabrication. However, until now, material lattice mismatch and incompatible thermal expansion coefficients between III–V materials and silicon substrates have fundamentally limited the monolithic growth of III–V lasers on silicon substrates by introducing high-density threading dislocations (TDs)[12].

Lasers with active regions formed from III-V quantum dots (QDs), nano-size crystals, can not only offer low threshold current density (J_{th}) but also reduced temperature sensitivity[13-17]. As shown in Figure 1a, within less than 10 years, the performance of QD lasers has surpassed state-of-the-art quantum-well (QW) lasers developed over the last few decades in terms of J_{th}. QD lasers have now been demonstrated with nearly constant J_{th}, output power (P_{out}), and differential efficiency at operating temperatures of up to 100 °C[18]. Very recently, III–V QD structures have drawn growing attention for the implementation of compound semiconductor lasers on silicon substrates[8-10,19]. This is because QDs have also been proved to be less sensitive to defects than conventional bulk materials and QW structures, due to carrier localization and hence a reduced interaction with the defects[20]. As shown in Figure 1b and c, a

[1]Department of Electronic and Electrical Engineering, University College London, London WC1E 7JE, United Kingdom, [2]Department of Electronic and Electric engineering, University of Sheffield, Sheffield, S1 3JD, United Kingdom, [3]Department of Physic and Astronomy, Cardiff University, Queens Building, The Parade, Cardiff, CF24 3AA, United Kingdom. *email: siming.chen@ucl.ac.uk; huiyun.liu@ucl.ac.uk

threading dislocation can only "kill" a very limited number of QDs, leaving the rest intact and able to provide optical gain. The enhanced tolerance to defects by localized states has also been witnessed in defect-insensitive nitride semiconductors, which are now used for the most efficient lighting technology[21]. More importantly, Figure 1b and c also reveal that the threading dislocation can be either pinned or propelled away from QDs. Therefore, the strong strain field of a QD array also prevents the in-plane motion of dislocations, and therefore superior reliability is expected from QD lasers compared with QW or bulk devices, even in the presence of high-density dislocations[22,23].

These unique properties of QDs provide a promising route towards monolithic III-V on silicon (III-V/Si) integration. As shown in Figure 1a, III-V QD lasers grown on silicon are rapidly approaching the performance of those grown on native GaAs substrates[24,25]. In addition, high-performance QD lasers have been successfully demonstrated on Ge-on-Si and Ge substrates, offering an albeit indirect route to III-V/Si integration[9,10,26]. However, it would be more attractive to realise a laser which did not require the intermediate germanium layer both because the requirement for the germanium layer restricts the range of silicon circuits to which it can be applied and since it is difficult to couple light through this layer to a silicon waveguide due to the high optical absorption coefficient of germanium at telecommunications wavelengths. Therefore, a high performance III-V laser directly grown on silicon is the preferred solution for silicon photonic-electronic integration.

Although QD lasers have demonstrated superior performance on silicon substrates in the last few years, our previous publications[8,24,25] indicate that epitaxially grown GaAs-on-Si substrates are much inferior when compared to bulk GaAs substrates in terms of total defect density, typically over 2×10^6 cm^{-2} compared with the order of 10^3-10^4 cm^{-2} for a GaAs substrate[27]. Furthermore, a high-performance electrically pumped continuous-wave (c.w.) QD laser directly grown on a silicon substrate has not yet been demonstrated. Here, by developing high-quality GaAs films with low TD density in the range of 10^5 cm^{-2}, we experimentally demonstrate high-performance 1310-nm InAs/GaAs QD lasers directly grown on silicon, with a record low J_{th}, high power, and high-temperature c.w. operation. Most significantly, a large number of operating hours with negligible degradation has been demonstrated for III-V lasers directly grown on silicon substrates for the first time.

In this work, InAs/GaAs QD lasers were directly grown on silicon substrates using a solid-source molecular beam epitaxy (MBE) system. In order to realize high-quality III–V lasers on silicon, it is necessary to minimize the impact of dislocations. Otherwise, TDs propagating into the active region will form nonradiative recombination centers and reduce minority-carrier lifetimes[23], leading to degradation of laser performance. To realize practical monolithic QD lasers with the performance and reliability necessary for monolithic integration, several strategies have been developed and employed in the current work. First, in order to prevent the formation of antiphase domains (APDs) while growing polar III-V materials on non-polar silicon substrates, phosphorus-doped Si(100) wafers with 4° offcut to the [011] plane were used[28] (FigureS1, Supplementary information I). A thin nucleation layer made of AlAs was deposited by migration enhanced epitaxy using alternating Al and As_4 flux at a low growth temperature of 350 °C. Figure 2a shows the high angle annular dark field scanning transmission electron microscopy (TEM) image of the interface. The thin AlAs nucleation layer has suppressed three-dimensional growth and provides a good interface for succeeding III-V material growth[19]. Following the AlAs nucleation layer, a three-step growth technique of GaAs epitaxial growth was performed[8,29]. The three layers of GaAs were grown at 350 °C, 450 °C, and 590 °C for 30 nm, 170 nm, and 800 nm, respectively. As shown in Figure 2b, most of the defects are well confined in the first 200 nm region thanks to the nucleation layer and multi-step temperature growth but still a high density (10^9 cm^{-2}) of TDs are seen to propagate towards the active region. To further improve the material quality, strained layer superlattices (SLSs) were grown as dislocation filter layers (DFLs) on the top of the GaAs buffer layer. Each SLS is made of five periods of 10-nm $In_{0.18}Ga_{0.82}As$/10-nm GaAs, which are repeated for four times separated by 300 nm GaAs spacing layers. The strain

relaxation of the SLSs applies an in-plane force to the TDs, which enhances the lateral motion of TDs considerably, and hence increases the probability for annihilation. *In-situ* thermal annealing of the SLS was also carried out four times, with the growth paused in the MBE reactor, by increasing the substrate temperature to 660 ^{o}C for 6 minutes. This approach can further improve the efficacy of filtering defects by increasing the mobility of the defects, leading to the defects annihilation before growth of the subsequent layers. As shown in Figure 2b and c, each set of $In_{0.18}Ga_{0.82}As$/GaAs SLSs can reduce the dislocation density by a few times. After the 300 nm GaAs spacer layers of the last SLSs, the dislocation density is reduced to the order of 10^5 cm^{-2} beyond the measurement capability of TEM. A typical atomic force microscopy (AFM) image for an uncapped QD sample grown on a silicon substrate with exactly the same conditions is shown in the inset of Figure 2d. A good QD uniformity is obtained with a density of ~3.0×10^{10} cm^{-2}. Based on the developed template, a standard 5-layer QD laser structure was then grown. A room temperature (RT) photoluminescence (PL) emission at around 1300 nm with a full width at half maximum (FWHM) of ~29 meV is also obtained, as shown in the Figure 2d, indicating a relatively small dot inhomogeneity. More uniformity studies of QDs grown on Si are presented in Figure S3 (Supplementary Information II). Cross-sectional scanning TEM measurements are used to characterize the QD active region grown on silicon substrates. The typical dot size is ~20 nm in diameter and ~7 nm in height, as shown in Figure 2e (top-left). The high-resolution high angle annular dark field scanning TEM images of a single dot also, to a large extent, show uniform In distribution with marginal intermixing as presented in Figure 2e (bottom-left). In addition, a nearly defect-free dot-in-well (DWELL) active region is observed, as shown in Figure 2e (right) and Figure S2 (Supplementary Information I).

Broad-area lasers were fabricated as shown schematically in Figure 3a. The lasers were processed with as-cleaved facets. A cross-sectional scanning electron microscope (SEM) image of a fabricated InAs/GaAs QD laser on a silicon substrate is shown in Figure 3b. It can be seen that a very clean and mirror-like facet has been achieved. This is important, because imperfectly cleaved facets result in increased mirror loss and reduced differential external quantum efficiency. No coatings were applied to the facets. An SEM overview of a complete III-V laser on silicon is shown in Figure 3c. Laser bars were then mounted on gold-plated copper heat-sinks using indium-silver low melting point solder and Au-wire bonded on the ridge to enable test (Supplementary Information III).

Low J_{th} and high optical P_{out} are always desirable goals for laser applications. Figure 4a shows the light-current-voltage (LIV) measurements for an InAs/GaAs QD laser grown on a silicon substrate under c.w. operation at RT. A clear knee behavior in the L-I curve is observed at the lasing J_{th} of 62.5 A/cm^2, which corresponds to 12.5 A/cm^2 for each of the five QD layers. To the best of our knowledge, this value of J_{th} represents the lowest c.w. RT J_{th} for any kind of laser on a silicon substrate to date, and is comparable to the best-reported values for conventional QD lasers on GaAs substrate[13,30]. The P_{out} measured from both facets is as high as 105 mW at an injection current density of 650 A/cm^2, with no evidence of power saturation up to this current density.

In many cases, the lasers exhibit non-linearity or 'kinks' in the above threshold LI characteristics. To understand the origin of this behavior, the evolution of emission spectra at various c.w. injection current densities is presented in Figure 4b. At a low injection of 50 A/cm^2, a broad spontaneous emission with a FWHM of 38 nm is observed at a peak wavelength of 1316 nm. As the current density increases to 62.5 A/cm^2, the peak at 1315 nm increases sharply in intensity and narrows to 2.4 nm, which is obvious evidence of lasing. Further increasing the injection current density gives rise to multi-mode lasing which becomes more pronounced at increasingly higher injection. Laser operation from the excited states is not observed up to the maximum injection of 650 A/cm^2, which indicates that those kinks observed in the LI curve are mainly related to mode competition and carrier redistributions between different modes within the ground state. This behavior is characteristic of the broad-area configurations and the non-linear effects are also observed

in the near-field of the laser which evolves with carrier injection (Supplementary Information IV).

In addition to J_{th} and P_{out}, for silicon photonic-electronic integration applications, it is important that lasers can operate at high temperature in c.w. mode. This is required because silicon-based electronic chips are often required to work in ambient temperature of 65 ^{o}C or even higher, without the use of thermo-electric cooling. Figure 4c shows the c.w. P_{out} for the QD laser at various temperatures. The c.w. lasing in the ground state was maintained until the testing was stopped at a heatsink temperature of 75 ^{o}C due to the limitation of the c.w. current source. This Si-based laser has also been tested under pulsed operation; lasing up to 120 ^{o}C is demonstrated with limited self-heating (Supplementary Information IV). To the best of our knowledge, this is the first demonstration of QD lasers directly grown on silicon substrates that lase up to 75 ^{o}C and 120 ^{o}C under c.w. and pulsed operation, respectively. The characteristic temperature T_0 for this device as estimated under pulsed operation is 51 K between 20 and 60 ^{o}C and 35K between 70 and 120 ^{o}C (Supplementary Information IV).

A critical requirement for the practical application of electrically pumped lasers on silicon is to achieve sufficient operating lifetime. High reliability, in terms of a long mean time to failure (MTTF) is an important pre-requisite to establish the feasibility of delivering commercial III-V QD lasers directly grown on silicon substrates. Here we present the results from our lifetime study on the InAs/GaAs QD laser epitaxially grown directly on a silicon substrate. The ageing test was performed at a fixed temperature of 26 ^{o}C, with the P_{out} monitored for a constant c.w. drive current of 210 mA (corresponding to $1.75\times I_{th}$). Periodic LIV characterizations were also performed to monitor changes in the lasing threshold. The ageing results are shown in Figure 4d. A 29.7% drop in power, over the ageing test period of 3,100 hours, is observed, with most of the drop (26.4%) occurring in the first 500 hours, followed by a very slow degradation of light output over time. A similar trend was observed for the threshold behavior, in which most of the increase in threshold occurred in the early stages of testing. An extrapolated MTTF (defined by a doubling of the threshold) of over 100,158 hours was determined from fitting the threshold with a sub-linear model (Supplementary Information V)[23]. It should be noted that these data represent worst case results since (i) the laser was operated epitaxial side up, (ii) the laser was not hard soldered to a high thermal conductivity heat-sink, and (iii) no facet coatings were used. Nevertheless, the estimated lifetime is much longer than the best reported extrapolated MTTF of 4,627 hours for a p-doped InAs/GaAs QD laser grown on Ge-on-Si 'virtual' substrate[23]. If the standard industrial techniques described above were used, even better lifetime performance is expected.

The realization of high-quality GaAs-on-silicon layers with low defects, by employing the combined strategies of AlAs nucleation layer, InGaAs DFLs, *in-situ* thermal annealing and utilizing QDs as laser active regions, developed using the MBE epitaxial growth method, represents a major step towards substituting III-V/Si epitaxy for the III-V on Ge and on Ge-on-Si 'virtual' substrates. Our results demonstrate that the large lattice mismatch between III-V materials and silicon will no longer be a fundamental hurdle for monolithic epitaxial growth of III-V photonic devices on silicon substrates. In particular, we have achieved c.w. lasing up to 75 ^{o}C, with an ultra low c.w. J_{th} of 62.5 A/cm^2, a high output power exceeding 105 mW at RT, and a long extrapolated lifetime of over 100,158 hours. Our demonstration of the ability to grow uniform high-quality III-V materials over the whole Si substrate and then fabricate electrically pumped lasers operating in c.w. mode to high temperature, with high uniformity and long lifetime, opens up new possibilities for silicon photonics and for the direct integration of optical interconnects on the silicon-based microelectronics platform.

Methods

Crystal growth. The epitaxial materials were fabricated by a solid-source Veeco Gen-930 molecular beam epitaxy system. Phosphorus-doped Si (100) wafer with 4° offcut to the [011]

plane was used. Prior to material growth, oxide desorption of silicon substrates was performed at 900 °C for 30 minutes. Epitaxy was then performed in the following order: a 6 nm AlAs nucleation layer, a 1 µm GaAs buffer layer, InGaAs/GaAs dislocation filter layers, five layers of InAs/GaAs DWELL structures separated by 50 nm GaAs spacers in the middle of a 140 nm undoped GaAs waveguide between 1.4 µm n-type lower and p-type upper $Al_{0.4}Ga_{0.6}As$ cladding layers. Each DWELL structure consisted of a layer of 3-monolayer InAs QDs sandwiched by 2 nm $In_{0.15}Ga_{0.85}As$ and 6 nm $In_{0.15}Ga_{0.85}As$. The DWELLs were grown at 510 °C and GaAs and AlGaAs layers at 590 °C. Finally, a 300 nm p-type GaAs contact layer was grown.

Device fabrication. The broad-area lasers with 50 µm wide stripes were fabricated by standard lithography and wet chemical etching techniques, the ridge was etched to roughly 100 nm above the active region, to give improved carrier confinement. Ti/Pt/Au and Ni/GeAu/Ni/Au were deposited on p^+-GaAs contacting layer and exposed n^+-GaAs buffer layer to form the p- and n- contacts, respectively. After lapping the silicon substrate to 120 microns, the lasers were cleaved to the desired cavity lengths and mounted (as-cleaved) onto the heat-sink.

Measurements. AFM measurements were performed with a Nanoscope Dimension™ 3100 SPM AFM system in ambient conditions using a noncontact mode. Conventional scanning TEM was performed using a JEOL 2010F field-emission gun TEM operating at 200 kV. Dislocation density measurements were derived from a series of bright field scanning TEM images using conventional inset-grid method and EELS to calculate the sample thickness. High-resolution high angle annular dark field Z-contrast scanning TEM images were acquired with a JEOL R005 aberration corrected TEM operating at 300 kV with a convergence semi-angle of 21 mrads and a TEM inner annular collection angle of 62 mrads. The reliability study was carried out in auto current control (ACC) mode at 26 ^oC under a constant c.w. current stress of 210 mA. The output power was collected from a photodetector normal to the laser facet, while periodic LIV measurements were taken to monitor the changes in lasing threshold. Other standard laser device characteristics were all measured under c.w. and pulsed conditions (1% duty-cycle and 1µs pulse-width).

References

1. M. Asghari, A. V. Krishnamoorthy, Silicon photonics: Energy-efficient communication. *Nature Photon.* **5**, 268-270 (2011).
2. A. Rickman, The commercialization of silicon photonics. *Nature Photon.* **8**, 579-582 (2014).
3. L. Virot *et al.*, Germanium avalanche receiver for low power interconnects. *Nature Commun.* **5**, 4957 (2014).
4. G. T. Reed, G. Mashanovich, F. Gardes, D. Thomson, Silicon optical modulators. *Nature Photon.* **4**, 518-526 (2010).
5. R. E. Camacho-Aguilera et al., An electrically pumped germanium laser. *Opt. Express* **20**, 11316-11320 (2012).
6. K. Tanabe, K. Watanabe, Y. Arakawa, III-V/Si hybrid photonic devices by direct fusion bonding. *Sci. Rep.* **2**, 349 (2012).
7. Z. Mi, J. Yang, P. Bhattacharya, D. Huffaker, Self-organised quantum dots as dislocation filters: the case of GaAs-based lasers on silicon. *Electron. Lett.* **42**, 121-123 (2006).
8. T. Wang, H. Liu, A. Lee, F. Pozzi, A. Seeds, 1.3-μm InAs/GaAs quantum-dot lasers monolithically grown on Si substrates. *Opt. Express.* **19**, 11381-11386 (2011).
9. A. Lee, Q. Jiang, M. Tang, A. Seeds, H. Liu, Continuous-wave InAs/GaAs quantum-dot laser diodes monolithically grown on Si substrate with low threshold current densities. *Opt. Express.* **20**, 22181-22187 (2012).
10. A. Liu *et al.*, High performance continuous wave 1.3 μm quantum dot lasers on silicon. *Appl. Phys. Lett.* **104**, 041104 (2014).
11. Z. Wang *et al*., Room-temperature, InP distributed feedback laser array directly grown on Silicon. *Nature Photon*.9, 837-842 (2015).
12. Z. Zhou *et al.*, On-chip light sources for silicon Photonics. *Light Sci. Appl.* **4**, e358 (2015).
13. D. Deppe, K. Shavritranuruk, G. Ozgur, H. Chen, S. Freisem, Quantum dot laser diode with low threshold and low internal loss. *Electron. Lett.* **45**, 54-56 (2009).
14. Y. Arakawa *et al.*, Multidimensional quantum well laser and temperature dependence of its threshold current. *Appl. Phys. Lett.* **40**, 939-941 (1982).
15. M. T. Crowley *et al*., in Semiconductors Semimetals: Advances Semiconductor Lasers, vol. 86. New York, NY, USA: Academic, ch. 10, 371–417 (2012).
16. D. Bimberg *et al*., Quantum Dot Heterostructures (John Wiley & Sons, Chichester, 1999).
17. G.T. Liu *et al*., Extremely low room-temperature threshold current density diode lasers using InAs dots in $In_{0.15}Ga_{0.85}As$ quantum well. *Electron. Lett.* **35**, 1163-1165 (1999).
18. M. Sugawara, M. Usami, Quantum dot devices: Handling the heat. *Nature Photon.* **3**, 30-31 (2009).
19. A. D. Lee *et al.*, InAs/GaAs Quantum-Dot Lasers Monolithically Grown on Si, Ge, and Ge-on-Si Substrates. *IEEE J. Sel. Top. Quantum Electron.* **19**, 1901107 (2013).
20. Z. Mi C. *et al.*, High-performance quantum dot lasers and integrated optoelectronics on Si. *Proc. IEEE* **97**, 1239-1248 (2009).
21. S. F. Chichibu *et al.*, Origin of defect-insensitive emission probability in In-containing (Al, In, Ga) N alloy semiconductors. *Nature Mater.* **5**, 810-816 (2006).
22. R. Beanland *et al.*, Structural analysis of life tested 1.3 μm quantum dot lasers. *J. Appl. Phys.* **103**, 014913 (2008).
23. A. Liu *et al.*, Reliability of InAs/GaAs quantum dot lasers epitaxially grown on silicon. *IEEE J. Sel. Topics Quantum Electron.* **21**, 1900708 (2015).
24. M. Tang *et al.*, 1.3-μm InAs/GaAs quantum-dot lasers monolithically grown on Si substrates using InAlAs/GaAs dislocation filter layers. *Opt. Express* **22**, 11528-11535 (2014).

25. S. Chen *et al.*, 1.3 μm InAs/GaAs quantum-dot laser monolithically grown on Si substrates operating over 100 C. *Electron. Lett.* **50**, 1467-1468 (2014).
26. H. Liu *et al.*, Long-wavelength InAs/GaAs quantum-dot laser diode monolithically grown on Ge substrate. *Nature Photon.* **5**, 416-419 (2011).
27. M. A. Tischler *et al*., Defect reduction in GaAs epitaxial layer using a GaAsP-InGaAs strained-layer superlattice. *Appl. Phys. Lett*. **46**, 294-296 (1985).
28. R. Fischer *et al*., Dislocation reduction in epitaxial GaAs on Si (100). *Appl. Phys. Lett*. **48**, 1223-1225 (1986).
29. M. Akiyama *et al*., Growth of single domain GaAs layer on (100)-oriented Si substrate by MOCVD. *Jpn. J. Appl. Phys.* **23**, L843 (1984).
30. I. Sellers *et al.*, 1.3 μm InAs/GaAs multilayer quantum-dot laser with extremely low room-temperature threshold current density. *Electron. Lett.* **40**, 1412-1413 (2004).

Acknowledgements

The authors acknowledge financial support from UK EPSRC under Grants No. EP/J012904/1 and EP/J012815/1. H.L. would like to thank The Royal Society for funding his University Research Fellowship.

Author contributions

H.L. proposed and guided the overall project with contributions from A.J.S. and P.M.S.. S.C., J.W., A.J.S., P.M.S. and H.L. developed the laser structure. J.W., M.T. and H.L. performed material growth. S.C. and Q.J. carried out the device fabrication and device characterization. S.S., S.N.E. and P.M.S. performed laser near-field measurements and analyses. A.S. and S.S. contributed to the development of device processing. W.L. and I.R. performed TEM characterization and analysis. M.T. and J.W. carried out AFM characterization. S.C., J.W., A.J.S. and H.L. composed the manuscript with input from all co-authors.

Additional Information

The authors declare no competing financial interests. Reprints and permission information is available online at http://npg.nature.com/reprintsandpermissions/. Correspondence and requests for materials should be addressed to H.L.

Competing financial interests

The authors declare no competing financial interests.

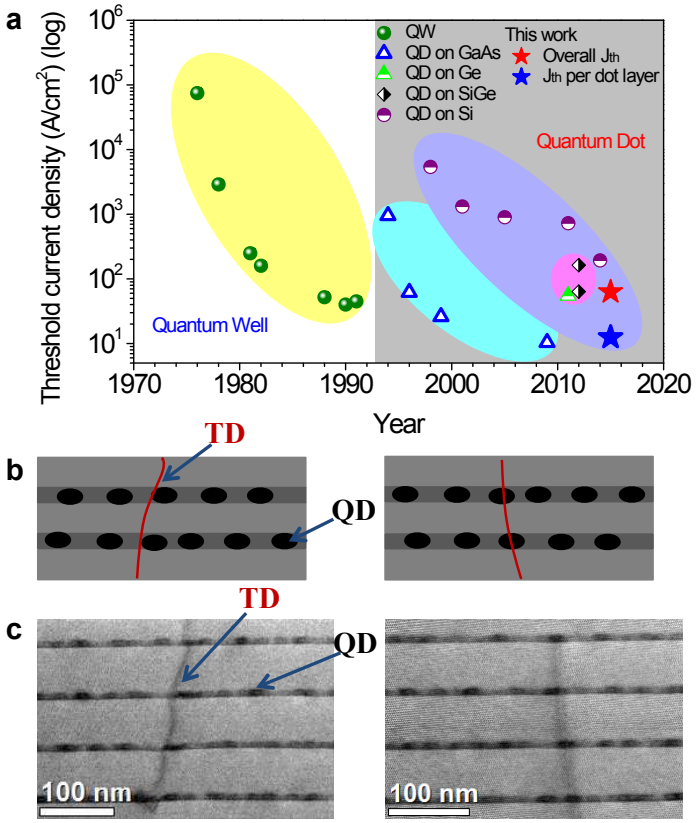

Figure 1. **Development and advantages of QD lasers**. (a) The historical development of low-dimensional heterostructure lasers showing the record threshold current densities. The red star indicates the threshold value achieved in this work. The blue star is the value normalized to a single QD layer. (b) Schematic of the interaction between QDs and threading dislocations. (c) Bright field scanning TEM images showing the potential interactions between threading dislocations and the QDs.

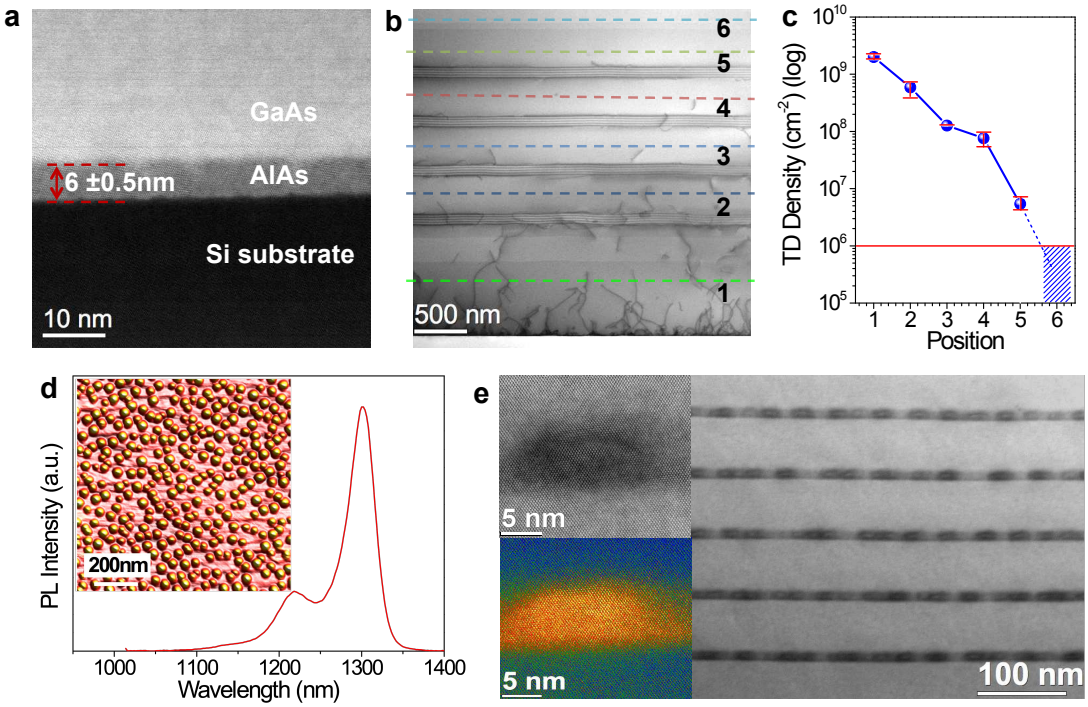

Figure 2. Epitaxial growth and structural characterization of QD lasers. (a) High angle annular dark field scanning TEM image of the interface between the 6 nm AlAs nucleation layer and a silicon substrate. (b) Bright field scanning TEM image of DFLs. (c) Dislocation density measured at different positions indicated in (b). (d) A PL spectrum for QD active region grown on silicon. The inset in (b) shows a representative AFM image of an uncapped QD sample grown on silicon. (e) High resolution bright field scanning TEM images of a single dot (top-left), corrected high angle annular dark-field scanning TEM images (false colour) of a single QD (bottom-left), and bright field scanning TEM image of the QD active layers (right).

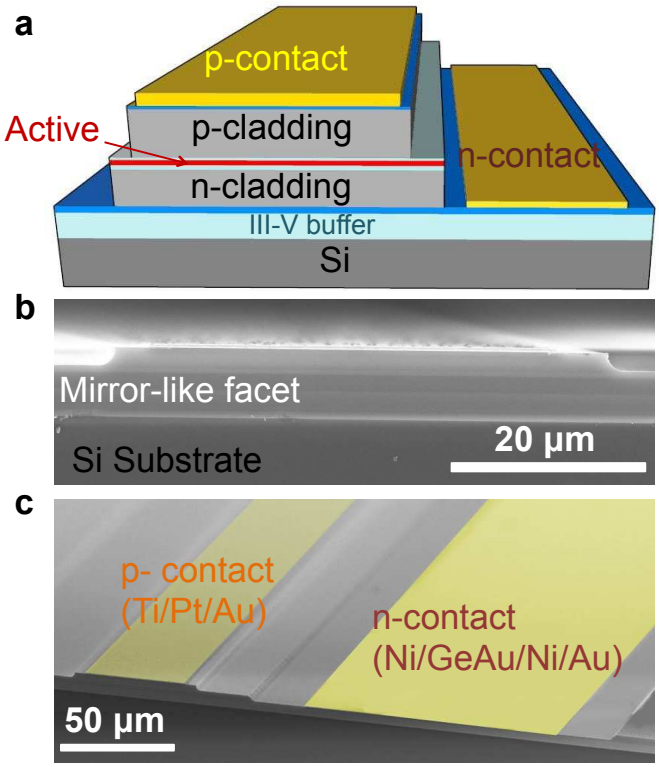

Figure 3. Fabricated III-V laser directly grown on silicon substrates. (a) Schematic of the layer structure of an InAs/GaAs QD laser on a silicon substrate. (b) A cross-sectional SEM image of the fabricated laser with as-cleaved facets, showing very good facet quality. (c) An SEM overview of whole III-V laser on silicon.

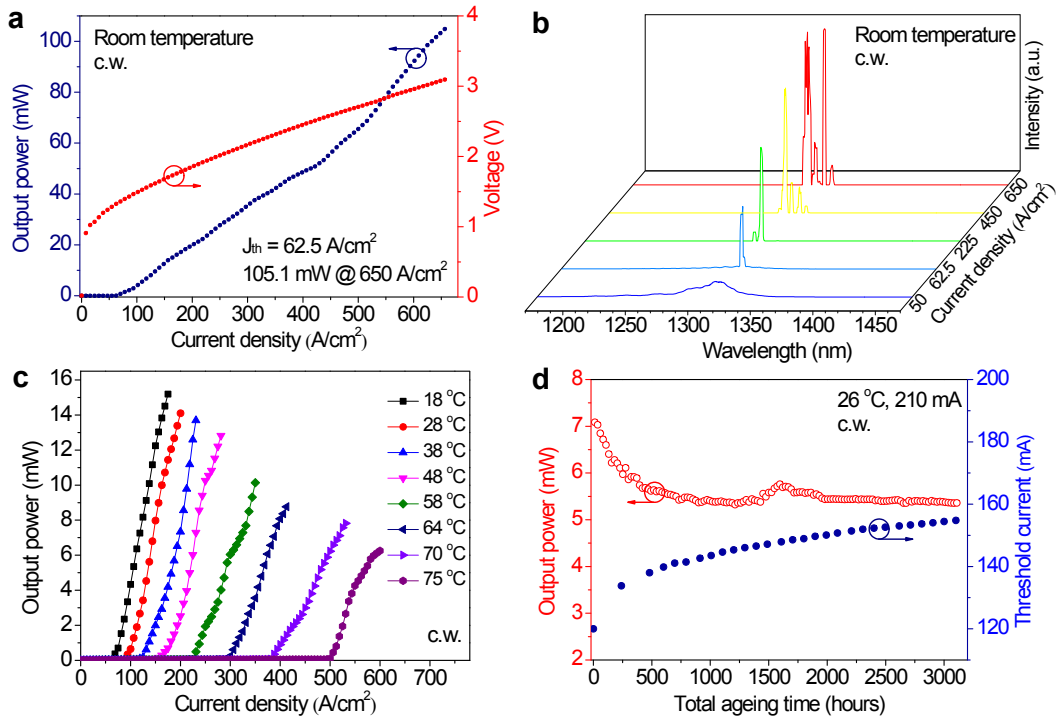

Figure 4. Silicon laser performance characterization. (a) LIV characteristics for a 50 μm × 3200 μm InAs/GaAs QD laser grown on a silicon substrate under c.w. operation at 18 °C. (b) Emission spectra for a 50 μm × 3200 μm InAs/GaAs QD laser grown on a silicon substrate at various injection current densities under c.w. operation at 18 °C. (c) Light output power versus current density for this InAs/GaAs QD laser on silicon at various heat sink temperatures. (d) Ageing data for InAs/GaAs QD laser on Si at constant heat sink temperature of 26 °C and c.w. drive current of 210 mA.